

High-resolution magnetostratigraphy of four sediment cores from the Greenland Sea—II. Rock magnetic and relative palaeointensity data

Norbert R. Nowaczyk^{1,*}

¹Fachbereich Geowissenschaften, Universität Bremen, Postfach 330440, D-28334 Bremen, Germany

Accepted 1997 June 17. Received 1997 June 17; in original form 1996 June 18

SUMMARY

High-resolution magnetostratigraphic analysis of three sediment cores from the base of the volcanic seamount Vesteris Banken in the Greenland Basin and one from the Jan Mayen Fracture Zone revealed records of three pronounced geomagnetic events: the Mono Lake excursion (28–27 ka), the Laschamp event (37–33 ka) and the Biwa I/Jamaica event (189–179 ka). Rock magnetic investigations, measurements of magnetic susceptibility, and ARM and IRM acquisition/demagnetization experiments show that only fine-grained (titano) magnetite ($\leq 0.5 \mu\text{m}$) is the dominant magnetic carrier mineral in the hemipelagic muds. There is no evidence for high amounts of high-coercivity minerals like haematite or goethite. Volcanic (basaltic) ash layers in sediments around Vesteris Banken seamount are characterized by extremely high values of magnetic susceptibility, reaching $16\,000 \times 10^{-6}$ (SI), as well as by low median destructive fields of the anhysteretic remanent magnetization (MDF_{ARM}), indicating magnetite of larger grain sizes ($\geq 1 \mu\text{m}$). Besides this, no significant variation in rock magnetic parameters across intervals of intermediate to reversed ChRM inclinations are observed. Therefore, these are interpreted as true records of geomagnetic field variations. The recovered sediments, characterized by only moderate fluctuations in concentration as well as grain-size-related rock magnetic parameters, provided good conditions for the reconstruction of the relative palaeointensity of the geomagnetic field. The recorded geomagnetic events are clearly linked to a drastic reduction in the relative palaeointensity of the field. The lowermost values were obtained for the time of the polarity transition with a trend to higher relative intensities in the course of the polarity events. Event ages and the relative palaeointensity variations, based on different methods, derived from the Greenland Sea sediments investigated are in good agreement with data published in the literature.

Key words: ARM, Brunhes Chron, IRM, palaeointensity, polarity reversals, rock magnetism.

INTRODUCTION

An increasing number of palaeomagnetic studies published during the last 10 years have focused on the palaeointensity of the geomagnetic field derived from different types of sediments (Tauxe & Valet 1989; Tauxe 1993; Guyodo & Valet 1996). The various relative palaeointensity records obtained show pronounced minima, which Valet & Meynadier (1993) related to geomagnetic excursions/short polarity events published in the

literature. Only a few of the published magnetostratigraphic data used for palaeointensity studies provide direct evidence for these high-frequency features of the geomagnetic field. Moreover, palaeomagnetic investigations performed on volcanic rocks have rarely succeeded in revealing geomagnetic excursions within the Brunhes Chron, one reason why their occurrence is still under discussion. However, these studies provided direct evidence that during these geomagnetic events the intensity of the geomagnetic field was reduced significantly (Roperch, Bonhommet & Levi 1988; Chauvin *et al.* 1989; Levi *et al.* 1990; Schnepp & Hradetzky 1994; Garnier *et al.* 1996).

Magnetostratigraphic analyses of deep-sea sediments recovered from the Norwegian–Greenland Sea and the Arctic

* Now at: GeoForschungsZentrum Potsdam, Projektbereich 3.3, Laboratory for Paleo- and Rock Magnetism, Telegrafenberg, D-14473 Potsdam, Germany. E-mail: nowa@gfz.potsdam.de

Ocean have consistently revealed the existence of several short-lived excursions or even full reversed intervals within the Brunhes Chron (Løvlie *et al.* 1986; Bleil & Gard 1989; Nowaczyk 1991; Nowaczyk & Baumann 1992; Nowaczyk *et al.* 1994). In this paper we discuss the rock magnetic results and relative palaeointensity records derived from four new cores recovered by R/V Polarstern from the base of Vesteris Banken and the Jan Mayen Fracture Zone in the Greenland Sea (Table 1). All four cores provide further evidence for three pronounced geomagnetic events: the Mono Lake excursion

Table 1. Location, water depth and length of sediment cores presented in this study.

Core number	Latitude	Longitude	Water depth	Length
PS 1707-2 KAL*	72°36.9'N	13°48.4'W	2122 m	530 cm
PS 1878-3 KAL	73°15.3'N	9°00.7'W	3048 m	469 cm
PS 1882-2 KAL	73°36.0'N	8°19.3'W	3175 m	650 cm
PS 1892-3 KAL	73°44.1'N	9°41.2'W	3002 m	436 cm

KAL: square-barrel Kastenlot corer (30 × 30 cm; KAL*: 15 × 15 cm)

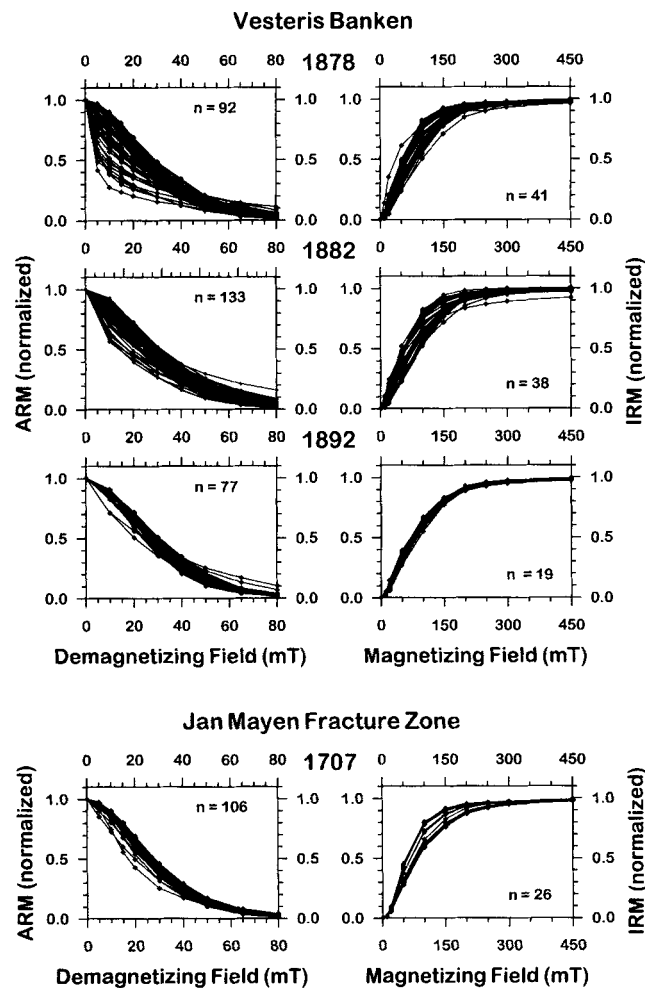


Figure 1. Normalized demagnetization curves of the anhysteretic remanent magnetization (ARM) and acquisition curves of the isothermal remanent magnetization (IRM) from the cores investigated. The IRM curves are normalized to the saturated IRM acquired at 1500 mT, defined as SIRM. For reasons of clarity the plots are cut off at 450 mT because all recorded curves reach saturation between 450 and 1000 mT. n denotes the number of samples investigated.

(Denham & Cox 1971) at 28–27 ka, the Laschamp event (Bonhommet & Babkine 1967) at 37–33 ka, and the Biwa I event (Kawai *et al.* 1972), also called the Jamaica event (Wollin *et al.* 1971), at 189–179 ka. A brief description of the recovered sediments, the sampling technique and a detailed discussion of the magnetostratigraphic results and the chronostratigraphic interpretation based on stable isotopes, $\delta^{18}\text{O}$ and $\delta^{13}\text{C}$, AMS ^{14}C dating (accelerator mass spectrometry) and foraminifera abundances is presented by Nowaczyk & Antonow (1997, this issue). In order to verify that the recorded intermediate and reversed directions reflect the true geomagnetic field behaviour, a rock magnetic investigation was performed on the cores. They were also investigated for the reconstruction of the palaeointensity of the geomagnetic field by normalizing the intensity of the natural remanent magnetization (NRM) by three different concentration-related parameters. The records obtained from the cores were transformed into time-series and compared with the high-resolution palaeointensity data reported in the literature (Meynadier *et al.* 1992; Tric *et al.* 1992; Valet & Meynadier 1993; Schneider 1993; Tauxe & Shackleton 1994; Roberts, Verosub & Negrini 1994; Stoner, Channell & Hillaire-Marcel 1995; Weeks *et al.* 1995; Guyodo & Valet 1996).

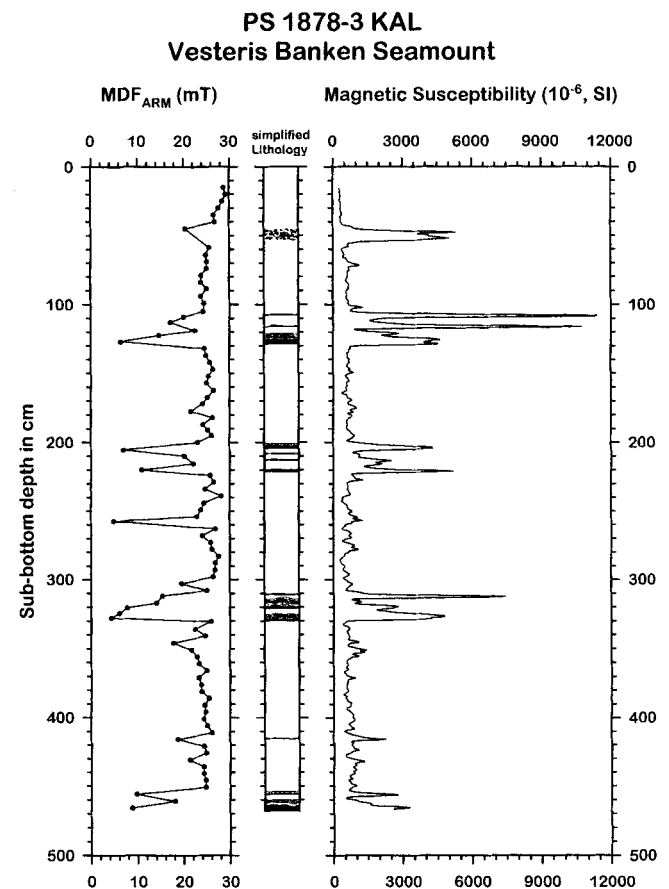


Figure 2. Core PS 1878-3 KAL: downcore variations of the median destructive field (MDF) of the anhysteretic remanent magnetization (ARM) (left), simplified lithology (middle) and high-resolution log of magnetic susceptibility (right). Extremely high susceptibilities as well as low MDF_{ARM} values correspond to coarse-grained volcanic ash layers indicated by grey and black stripes in the lithology log.

ROCK MAGNETIC INVESTIGATIONS

In order to check for relative changes in mineral magnetic parameters and to verify the palaeomagnetic information, all samples from the four cores discussed by Nowaczyk & Antonow (1997) in the accompanying paper were subjected to rock magnetic analysis. The measurements were performed at the new Laboratory for Paleo- and Rock Magnetism of the GeoForschungsZentrum (GFZ), Potsdam, Germany. A

Bartington MS2B sensor was used to determine the magnetic susceptibility κ of all palaeomagnetic samples at 460 Hz (low-frequency κ , κ_{LF}) and 4600 Hz (high-frequency κ , κ_{HF}). Measurements of the anhysteretic remanent magnetization (ARM) intensities were measured with a fully automated 2G Enterprises DC-SQUID 755 SRM long-core system with an in-line triaxial degausser. Before imprinting the ARMs, the samples were demagnetized in a field of 150 mT AF amplitude using the integrated three-axis degausser of the 2G 755 SRM.

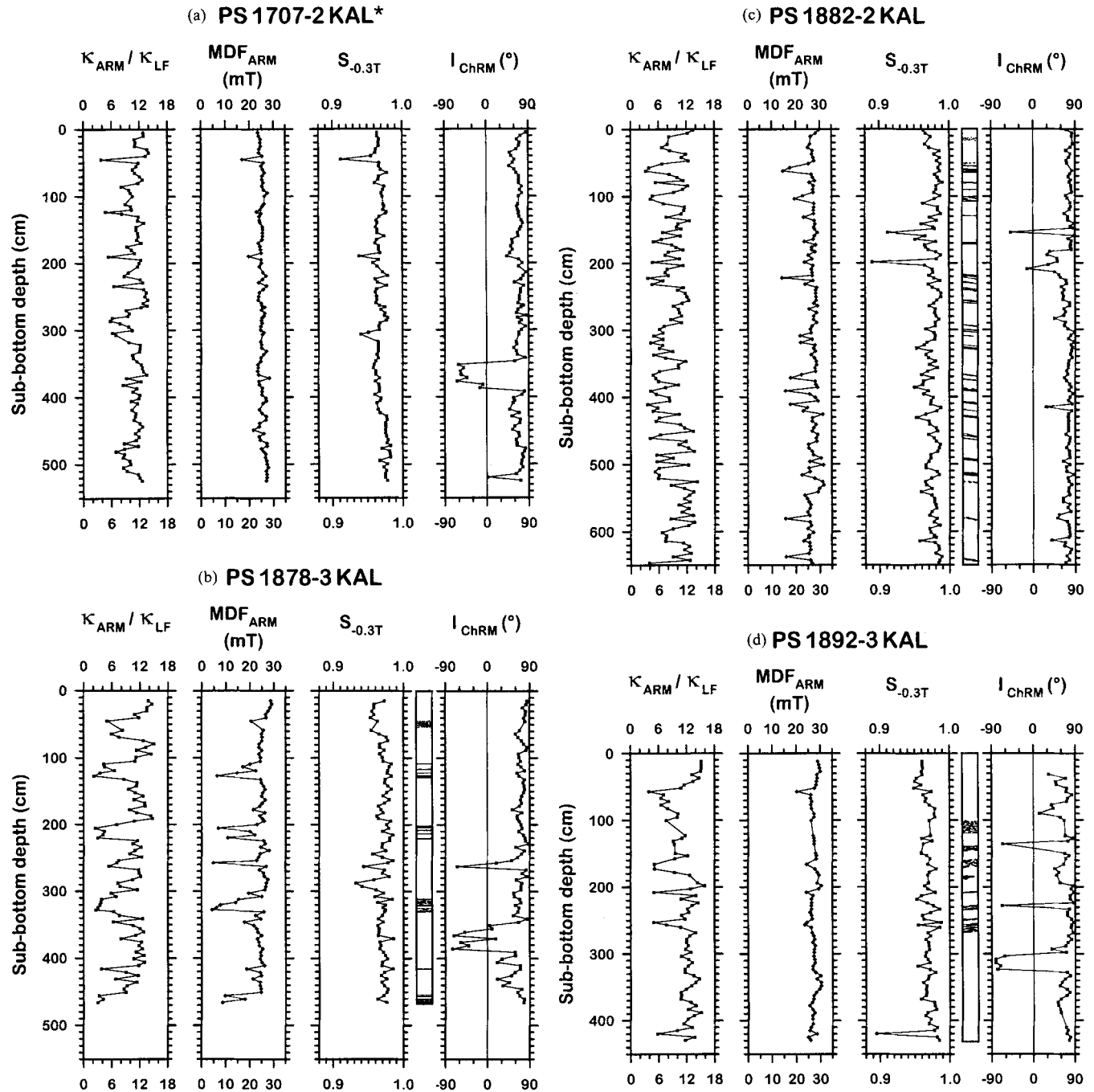


Figure 3. Downcore variations of rock magnetic parameters of the cores from the Jan Mayen Fracture Zone and around Vesteris Banken Seamount, Greenland Sea. Grain-size-related parameters: κ_{ARM}/κ_{LF} = anhysteretic susceptibility divided by low-field magnetic susceptibility; κ_{LF} = low-field magnetic susceptibility at 460 Hz; κ_{ARM} = ARM divided by the strength of the dc field used for acquisition; MDF_{ARM} = median destructive field of the ARM. Mineralogy-related parameters: $S_{-0.3T} = 0.5 \times (1 - [IRM_{-0.3T}/SIRM])$; $IRM_{-0.3T}$ = IRM after demagnetizing SIRM by a reversed field of -0.3 T. Palaeomagnetic data: I_{ChRM} = inclination of the characteristic remanent magnetization.

ARMs were produced along the positive z-axis of the samples with a 0.05 mT static field and a 100 mT AF amplitude using a separate 2G Enterprises 600 single-axis demagnetizer including an ARM coil (maximum static field 1 mT). The ARM intensities of the samples were then measured and demagnetized with the 2G 755 SRM at AF levels of 0, 5, 10, 15, 20, 30, 40, 50, 65 and 80 mT. The resulting demagnetization curves are displayed in Fig. 1. The median destructive fields (MDF_{ARM}) of core PS 1707-2 KAL* range from 17.1 to 28.3 mT, with only three MDF_{ARM} values below 24 mT. This indicates a fairly homogenous coercivity spectrum throughout the core, with stable magnetite as the main remanence carrier. A similar result was obtained for core PS 1892-3 KAL. The broadest MDF_{ARM} range, 4.3–29.2 mT (Fig. 1), was obtained for core PS 1878-2 KAL, reflecting the quite heterogeneous lithology, from hemipelagic muds (clay fraction) to coarse-grained basaltic ashes (sand fraction). Low MDFs are restricted to the basaltic ash layers with high magnetic susceptibilities, as seen in Fig. 2, whereas MDF_{ARM} values of the fine-grained hemipelagic muds are not lower than 25 mT.

Isothermal remanent magnetizations (IRM) were imprinted with a 2G Enterprises 660 pulse magnetizer (maximum peak field 2.7 T). Measurements of the IRM intensities were carried out with a Molyneux MiniSpin fluxgate magnetometer (noise level $0.2 \times 10^{-3} \text{ A m}^{-1}$) driven by GFZ software. Representative portions of the sample collection were exposed stepwise to peak fields of 10, 20, 50, 100, 150, 200, 250, 300, 450, 700, 1000 and 1500 mT along the positive z-axis of the samples in order to record complete IRM acquisition curves. The remainder of the sample collection was only exposed to a

field of 1500 mT. Although the pulse magnetizer is able to produce higher fields, a level of 1500 mT was chosen because otherwise the coil would have heated up too much if the magnetizing pulse was triggered as fast as the instrument was able to respond (about every 45 s for 2.7 T). Moreover, all recorded IRM acquisition curves reached saturation between 450 and 1000 mT (Fig. 1) and therefore do not show evidence for larger amounts of high-coercivity minerals like haematite or goethite. The IRM acquired at 1500 mT is therefore defined as the 'saturation' isothermal remanence (SIRM). The median acquisition fields (MAF) range from 37.2 to 99.3 mT for core PS 1878-3 KAL (maximum variations) and from 71.2 to 91.5 for core PS 1892-3 KAL (minimum variations).

After applying a field of 1500 mT all samples were magnetized with a field of 300 mT in the opposite direction. The resulting IRM intensity should be due only to high-coercivity anti-ferromagnetic minerals, because even the hardest ferrimagnetic particles would be remagnetized in a field of 300 mT. Single-domain titanomagnetite can have higher coercivities, that is hysteresis has not yet closed. The fraction of high-coercivity magnetominerals present can be estimated by calculation of the ratio

$$S_{-0.3T} = \frac{1}{2} \left(1 - \frac{IRM_{-0.3T}}{SIRM_{1.5T}} \right),$$

which ranges from 0 for pure haematite or goethite to 1 for pure magnetite (Bloemendahl *et al.* 1992).

The most significant results of the rock magnetic studies, together with the ChRM inclinations of the four cores

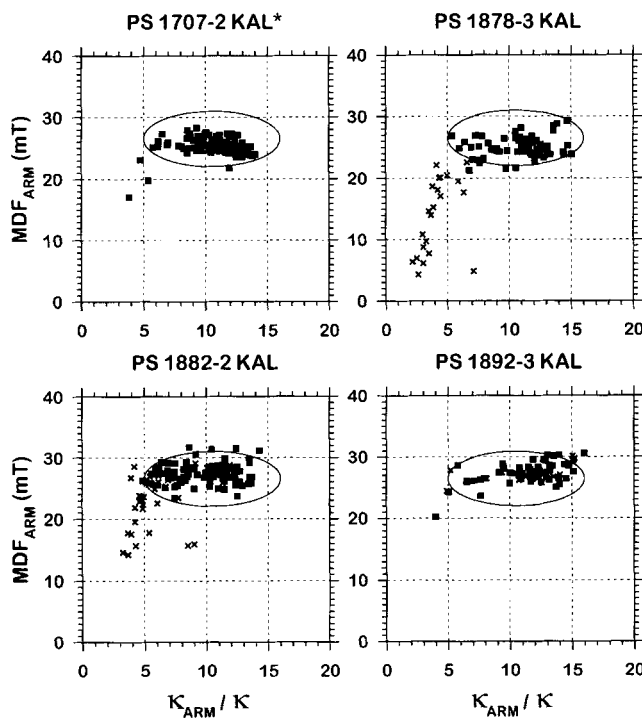


Figure 4. Median destructive field of the anhysteretic remanent magnetization (MDF_{ARM}) versus the ratio κ_{ARM}/κ_{LF} . Almost all samples from fine-grained hemipelagic muds (squares) plot within the area indicated by the ellipses in the diagrams, whereas samples from coarse-grained ash layers (crosses) show a linear increase of MDF_{ARM} with increasing κ_{ARM}/κ_{LF} ratio.

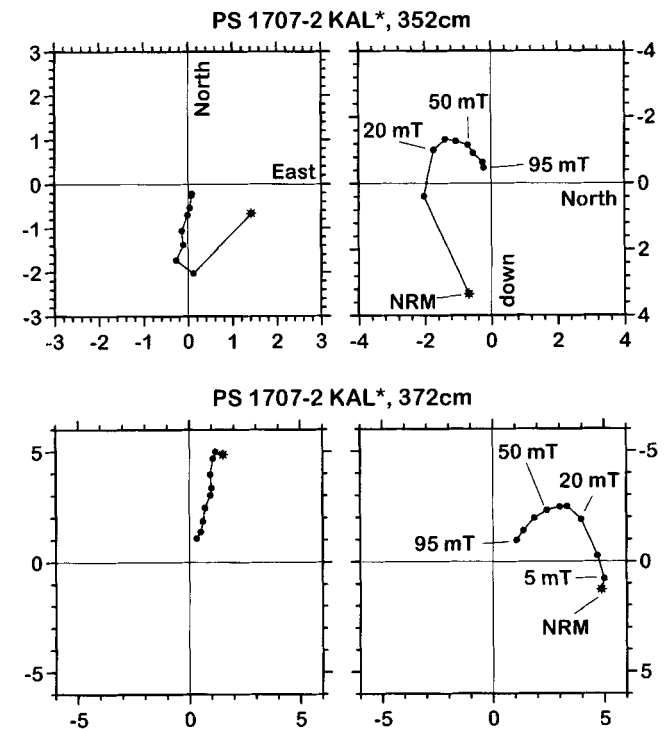


Figure 5. Zijderveld diagrams of two samples from core PS 1707-2 KAL* from the Jan Mayen Fracture Zone. Horizontal plane (left); vertical plane in the north/south direction (right). In both samples a steep normal overprint is eliminated with AF amplitudes of up to 50 mT until the negative ChRM inclination is completely isolated. Axis scaling is in mA m^{-1} .

investigated, are presented in Fig. 3 as a function of sub-bottom depth. The parameter κ_{ARM} , which is defined as ARM intensity divided by the amplitude of the static field used for its acquisition, is referred to as ‘anhysteretic susceptibility’. The ratio of anhysteretic susceptibility to low-field susceptibility

$\kappa_{\text{ARM}}/\kappa_{\text{LF}}$ (King *et al.* 1982) is indicative of grain size, because the trend of each parameter is in the opposite sense with increasing grain size. High ratios represent fine-grained particles, whereas low ratios are indicative of coarse-grained particles. The median destructive fields of the anhysteretic

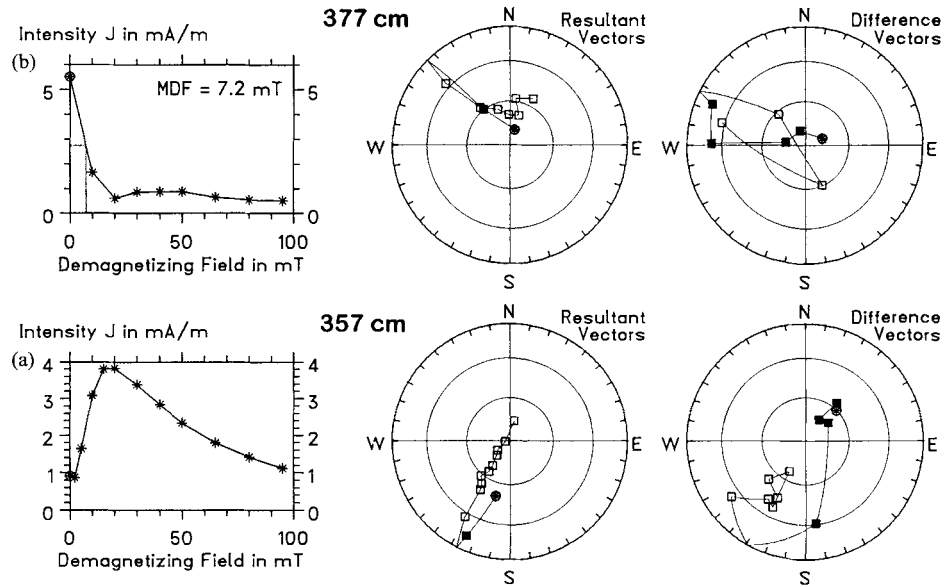


Figure 6. Demagnetization curves and equal-area stereographic projections of the resultant vectors and difference vectors of two samples from core PS 1707-2 KAL*.

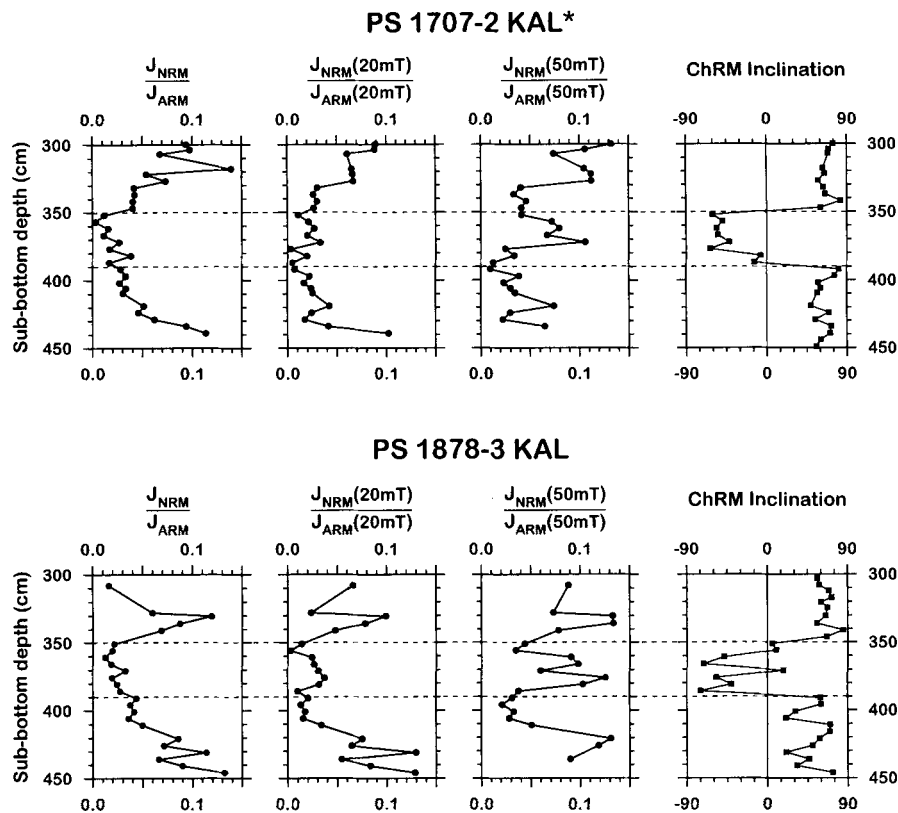


Figure 7. NRM/ARM ratios at three different demagnetization levels together with the ChRM inclination records showing the Laschamp event for cores PS 1707-2 KAL* and PS 1878-3 KAL in the sub-bottom depth interval of 300–450 cm. The results clearly indicate a pronounced low in relative palaeointensity during the N–R and R–N transitions of the geomagnetic field and a slight recovery of the intensity in the middle of the Laschamp event. This pattern is only visible after complete removal of normal-polarity overprints with at least 50 mT AF treatment (*cf.* Fig. 6).

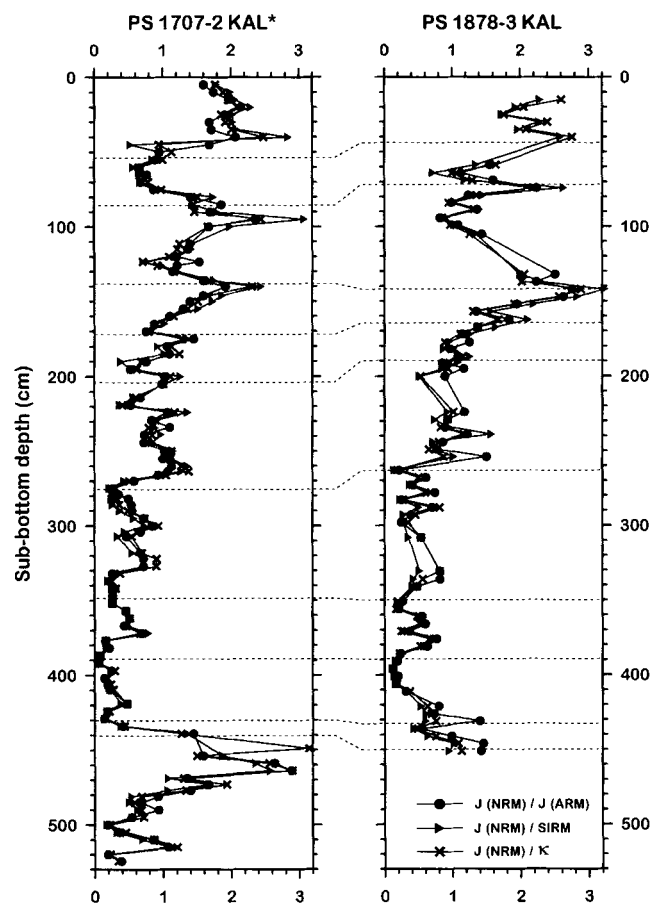


Figure 8. Correlation and palaeointensity approximation of cores PS 1707-2 KAL* and PS 1878-3 KAL calculated by three different methods. In order to compare the results, all three curves for each core have been normalized to their individual averages. In general, the resulting variations are indistinguishable from each other.

remanent magnetization (MDF_{ARM}) for hemipelagic muds from all cores are independent of the ratio κ_{ARM}/κ_{LF} (squares surrounded by ellipses in Fig. 4). Most of the samples from coarse-grained ash layers (crosses in Fig. 4) show a linear increase of MDF_{ARM} with increasing κ_{ARM}/κ_{LF} ratio. κ_{ARM}/κ_{LF} ratios of about 5–16 obtained for hemipelagic muds in the cores, as indicated by the ellipses in Fig. 4, correspond to fine-grained magnetite of about $\leq 0.5 \mu\text{m}$ (Bloemendahl *et al.* 1992). Ash layers in cores from Vesteris Banken exhibit significantly lower κ_{ARM}/κ_{LF} ratios of down to 3, indicating magnetite of $> 1 \mu\text{m}$ grain size. Further evidence for magnetite as the main magnetic mineral is provided by $S_{-0.3 \text{ T}}$ ratios, which show small dispersions around a value of 0.97, indicating a fairly constant and small contribution (maximum ≈ 10 per cent) of high-coercivity minerals to the magnetization in the cores investigated (Bloemendahl *et al.* 1992).

In summary, the intermediate to reversed inclinations linked to the Laschamp event recorded from 350 to 390 cm in core PS 1707-2 KAL are situated within an interval of homogenous grain-size- and mineralogy-related rock magnetic properties. The same is true of the Laschamp event from 350 to 390 cm in core PS 1878-3 KAL and of the Biwa 1/Jamaica event recorded from 300 to 325 cm in core PS 1892-3 KAL. Core PS 1882-2 KAL is characterized by a larger scatter of the κ_{ARM}/κ_{LF} ratios through the whole core, which might explain

the incomplete recording of the Laschamp event and the absence of older events such as the Blake. However, the scatter of κ_{ARM}/κ_{LF} ratios still lies within the range of the hemipelagic muds of the other cores. So, in general, the palaeomagnetic signatures of all cores are mainly independent of magnetomineralogy.

RELATIVE PALAEOINTENSITY RECORDS

Choice of demagnetization level

During the NRM demagnetization of samples with a reversed ChRM magnetization, a low-coercivity component of normal polarity was generally removed at the first AF levels. The orthogonal diagrams in Fig. 5 show two examples of such samples from core PS 1707-2 KAL*, both with negative ChRM inclinations but one with a northerly and the other with a southerly ChRM declination. In both cases a level of 50 mT was necessary to completely eliminate the viscous overprint. If the overprint is oriented antiparallel to the ChRM component the resultant NRM intensity is significantly reduced and shows an initial increase during the first demagnetization steps. The intensity of sample 357 cm in Fig. 6(a) increases by a factor of about 4 at 20 mT AF peak amplitude. In this case the vector component of the normal-polarity overprint was almost the same as the remaining high-coercivity reversed-polarity component. If the amount of antiparallel normal-polarity overprint is larger than the high-coercivity reversed-polarity component (sample 377 cm, Fig. 6b), then the intensity first decreases until both components are more or less the same (here at 20 mT), then increase until the overprint is removed (here at 50 mT) and finally decreases again as the high-coercivity component is removed. Fig. 7 shows how relative palaeointensity records depend on the choice of demagnetization level. The NRM intensities of cores PS 1707-2 KAL* and PS 1878-3 KAL were divided by the ARM intensities and then normalized to their averages. Fig. 7 displays the NRM/ARM ratios without demagnetization, after treatment with 20 mT and 50 mT, together with the ChRM inclination for the depth interval 300–450 cm, with the Laschamp event documented in the middle. The morphologies of these intervals exhibit significant modulations with progressive demagnetization, caused by the removal of the normal-polarity overprint. The most striking effect is the increase in the NRM/ARM ratio for the central section of the Laschamp event in both cores until treatment with 50 mT, while the ratio stays at lower values for the N–R and R–N transitions. In order to avoid the influence of a remaining partial normal-polarity overprint in intervals of reversed or intermediate ChRM directions, the NRM intensity after treatment with 50 mT [$J_{NRM}(50 \text{ mT})$] was chosen as a database for the calculation of all relative palaeointensity records. Using 20 mT, as has been done in most of the published palaeointensity studies performed on sediments, would have led to an underestimation of the field amplitude in the case of the Greenland Sea sediments.

Choice of normalization method

To approximate the relative palaeointensity for the sediments investigated, the values of $J_{NRM}(50 \text{ mT})$ were divided as follows:

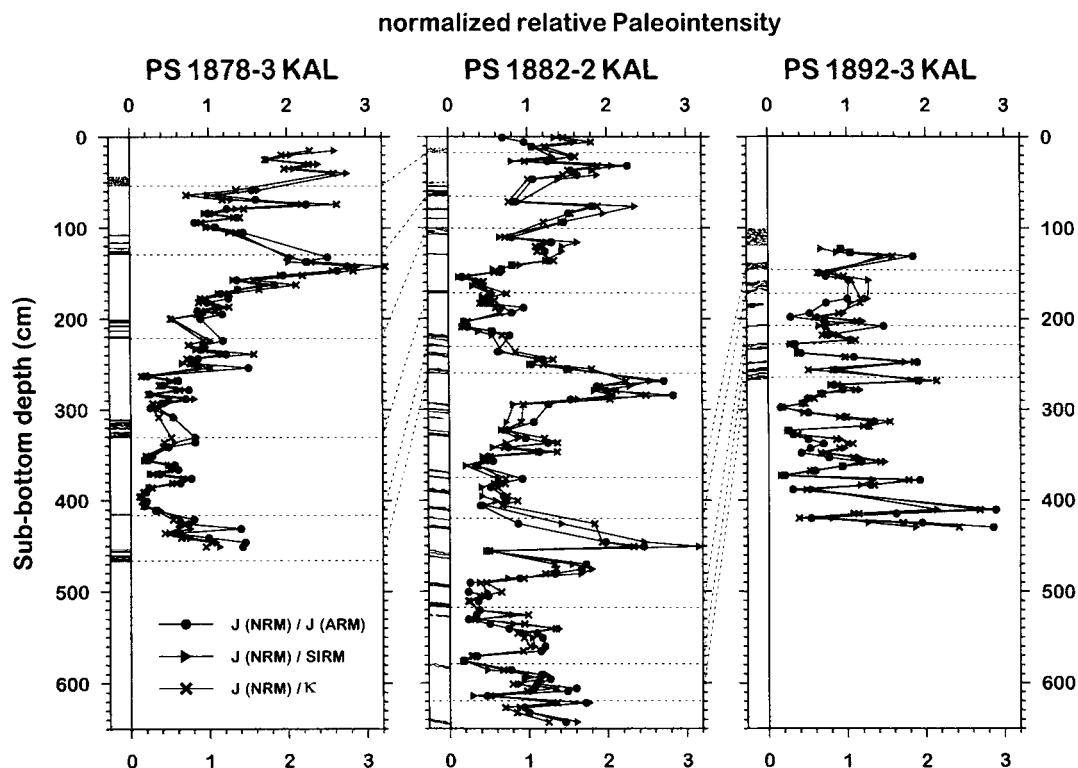


Figure 9. Correlation and palaeointensity approximation of Vesteris Banken cores, sites PS 1878, 1882 and 1892, calculated by three different methods. The dashed lines indicate the correlation of the cores derived from high-resolution logging of magnetic susceptibility, AMS¹⁴C dating, stable isotope stratigraphy ($\delta^{18}\text{O}$, $\delta^{13}\text{C}$) and biostratigraphy (Nowaczyk & Antonow 1997, this issue). Ash layers are indicated by simplified lithology logs. Because of strongly deviating rock magnetic parameters, samples from, or containing, these ash layers were not included for palaeointensity approximation.

(1) by the ARM-intensities of the same demagnetization level: $J_{\text{NRM}}(50)/J_{\text{ARM}}(50)$;

(2) by the SIRM: $J_{\text{NRM}}(50)/\text{SIRM}$; and

(3) by the low-field magnetic susceptibility: $J_{\text{NRM}}(50)/\kappa_{\text{LF}}$,

and then normalized to their averages. Because of their strongly deviating magnetic properties, samples taken from ash layers (see Figs 3 and 4) have been omitted from the calculation so that the data sets are based only on samples from hemipelagic muds with homogenous rock magnetic parameters. The results are presented in Figs 8 and 9. The morphologies of the three curves derived are almost the same for each core, independent of the method of normalization. For further data processing, $J_{\text{NRM}}(50 \text{ mT})/J_{\text{ARM}}(50 \text{ mT})$ was chosen. The ARM mainly affects fine-grained magnetite particles that are also the carriers of the palaeomagnetic information, whereas κ_{LF} and SIRM are also influenced by multidomain particles that do not contribute to a stable NRM. The age models for the four cores discussed by Nowaczyk & Antonow (1997, this issue) were used to calculate the time-dependent relative palaeointensities (Fig. 10). Because the correlation of the cores is mainly based on continuous magnetic susceptibility data measured every 5 mm, but the palaeo- and rock magnetic data are based on discrete samples taken every 5 cm, it seemed to be useful to combine the data sets to produce one curve by sorting the calculated ages. In this way, assuming a correct correlation, the data density with respect to time for the composite curve should be better than for each individual core. The different

time resolutions and time coverages did not allow a stacking of the curves. For the same reason, and also because of variations in the data quality, the palaeomagnetic results, ChRM inclination and ChRM declination logs are simply superimposed in Fig. 10.

DISCUSSION

The composite curve in Fig. 10 shows that the relative intensity decreased from a pronounced maximum at 45 ka to a broad minimum at the onset of directional variations of the Laschamp event at 37 ka. The intensity remained at relatively low values until the termination of the Mono Lake excursion at 27 ka. The increase in palaeointensity in the middle of the Laschamp event might be interpreted as a slight consolidation of the reversed-polarity state, but the relative amplitudes are still far below the values obtained for sediments at 250, 150, 100 and 45 ka and younger than 20 ka (Fig. 10). Allowing for age shifts of up to 3 ka in the Vesteris Banken data, a correlation with the palaeointensity stack of Meynadier *et al.* (1992), based on data from the Mediterranean Sea (Tric *et al.* 1992) and the Indian Ocean, yields some general similarities but also some large deviations (Fig. 11). In particular, for the time window spanning the period from the onset of the Laschamp event (37 ka) to the termination of the Mono Lake excursion (27 ka) the curves are different. No maximum was determined at 32.5 ka. Sediments from the Sulu Sea also yielded an intensity low from 45 to 30 ka (Schneider & Mello 1996), showing a general congruence with the Greenland Sea data (Fig. 11). The

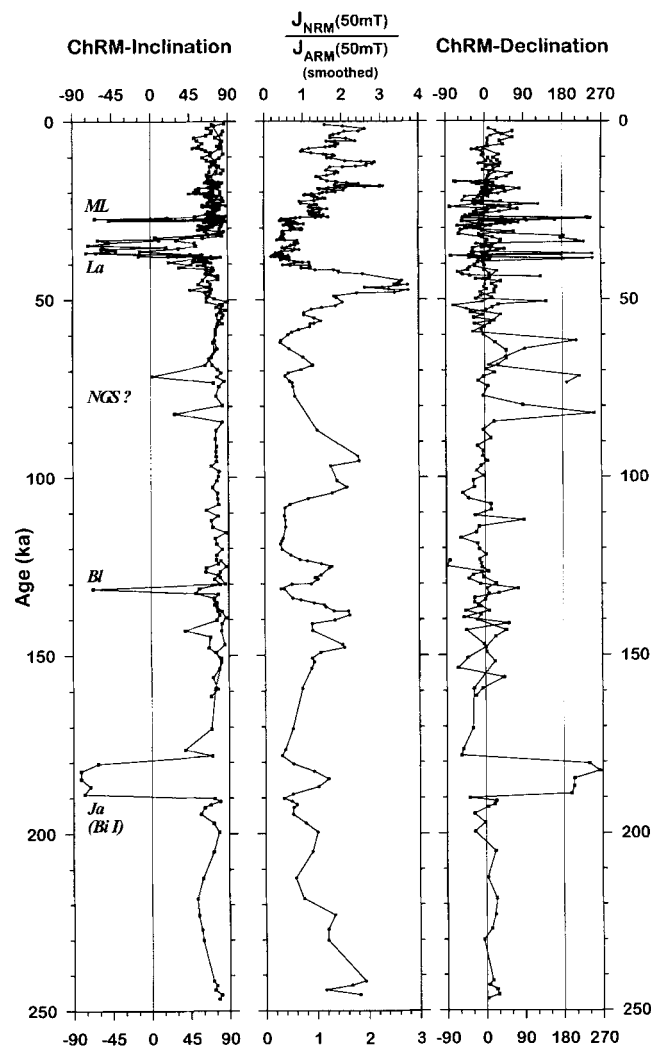


Figure 10. Relative palaeointensities, $J_{\text{NRM}}(50 \text{ mT})/J_{\text{ARM}}(50 \text{ mT})$ (middle), ChRM inclinations (left) and ChRM declinations (right) versus age as derived from sites PS 1707, 1878, 1882 and 1892 in the Greenland Sea. The palaeointensity composite was achieved by sorting the individual logs with respect to time. For the display the curve has been smoothed with a three-point weighted running average (triangular window). The directional data are simply superimposed because of the different data quality. Magnetostratigraphic data from Nowaczyk & Antonow (1997, this issue). Reversals of the geomagnetic field, unequivocally recognizable from steep negative inclinations, are clearly linked to lows in the palaeointensity, especially during the polarity transitions, with a slight to moderate intensity recovery in the middle of the longer events. The polarity events are labelled as follows: ML—Mono Lake; La—Laschamp; NGS—Norwegian–Greenland Sea; BI—Blake; Ja—Jamaica; Bi I—Biwa I.

palaeointensity stack from Ontong–Java Plateau sediments (Tauxe & Shackleton 1994) also shows pronounced minima at 40 and 20 ka, with a small relative minimum at 28 ka. However, relative palaeointensity data based on cores from the Labrador Sea (Stoner *et al.* 1995), which were recovered between about 50° and 58°N, closer to the Greenland Sea sites, are more like the Mediterranean/Indian Ocean stack of Meynadier *et al.* (1992). Stoner *et al.* (1995) discussed dating discrepancies between the two stacks of up to c. 10 ka. They also obtained a pronounced maximum around 45–50 ka, a feature that is

present in all other published data (Tauxe 1993) and a minimum in palaeointensity at 20 ka. No geomagnetic excursion linked to this intensity minimum has been recorded in the sediments investigated and only one paper (Thouveny 1988) records an excursion at 18 ka (Nowaczyk *et al.* 1994).

A stack based on 18 published palaeointensity records of Guyodo & Valet (1996) shown in Fig. 11, together with its error bars, shows the general features of the last 70 ka: an intensity maximum from 60 to 50 ka, a minimum around 40 ka and then an almost linear increase until the present. Deviations of the relative palaeointensities derived from different sites for the time span 45–25 ka, as discussed above, may imply that the geomagnetic field has been characterized more by the influences of multipoles than by the dipole moment.

Because of lower sedimentation rates, a hiatus and some disturbance of its top, core PS 1892–3 KAL yielded only a low-resolution record of palaeointensity for the time interval back to 250 ka. Nevertheless, this core yielded quite interesting results on the geomagnetic field behaviour across the Biwa I/Jamaica event at 189–179 ka (Fig. 10). The N–R as well as the R–N swings of ChRM inclinations and declinations are associated with a clear minimum in the relative palaeointensity record, whereas the full reversed directions exhibit relative intensity amplitudes almost reaching the amplitudes of the intensity maximum at 250, 150, 100 and 45 ka (Fig. 11). The intensity maximum during the Biwa I/Jamaica event is not situated in the middle of the event but shifted to older ages. Such a pattern, although only about 10 ka in duration, is more typical of a stable dipole configuration such as the Kaena and Mommoth events during the Gauss Chron (*cf.* Valet & Meynadier 1993) than of a polarity excursion. This might indicate that the convection processes in the Earth's outer core generating the geomagnetic field went into a stable state for a short time. A similar intensity pattern for the time interval covered by the Biwa I/Jamaica event is presented by Weeks *et al.* (1995) for sediment cores recovered from the North Atlantic. Core SU9008 in their study also exhibits clear directional deviations from the expected dipole directions in the time interval 190–175 ka (Fig. 7 in Weeks *et al.* 1995).

With the background of relative palaeointensity curves summarized by Guyodo & Valet (1996), together with data on Brunhes Chron events, the term 'stable normal polarity' now appears in a different light. All these data sets imply that the geomagnetic field has a much more dynamic character than would be expected from the polarity timescale, such as that of Cande & Kent (1995), which represents only the sign of the Earth's magnetic dipole moment throughout time.

The quality of geomagnetic variations recorded in sediments is influenced by a variety of rock magnetic parameters, for example concentration, granulometry, magnetomineralogy, coercivity spectrum, as well as by properties of the sediment matrix such as the depositional environment, the grain-size distribution, the grain shape, the degree and kind of bioturbation and post-depositional chemical processes. The optimal combination of all these factors is obviously not realized for all sediments and environments so that the high-frequency directional variations associated with geomagnetic events throughout the Brunhes Chron have been preserved in sediments at only a few sites (Nowaczyk *et al.* 1994). This may also explain the absence of the Blake event (Smith & Foster 1969) and the Norwegian–Greenland Sea event (Bleil & Gard 1989) at about 120 ka and 75 ka, respectively, in the cores investigated.

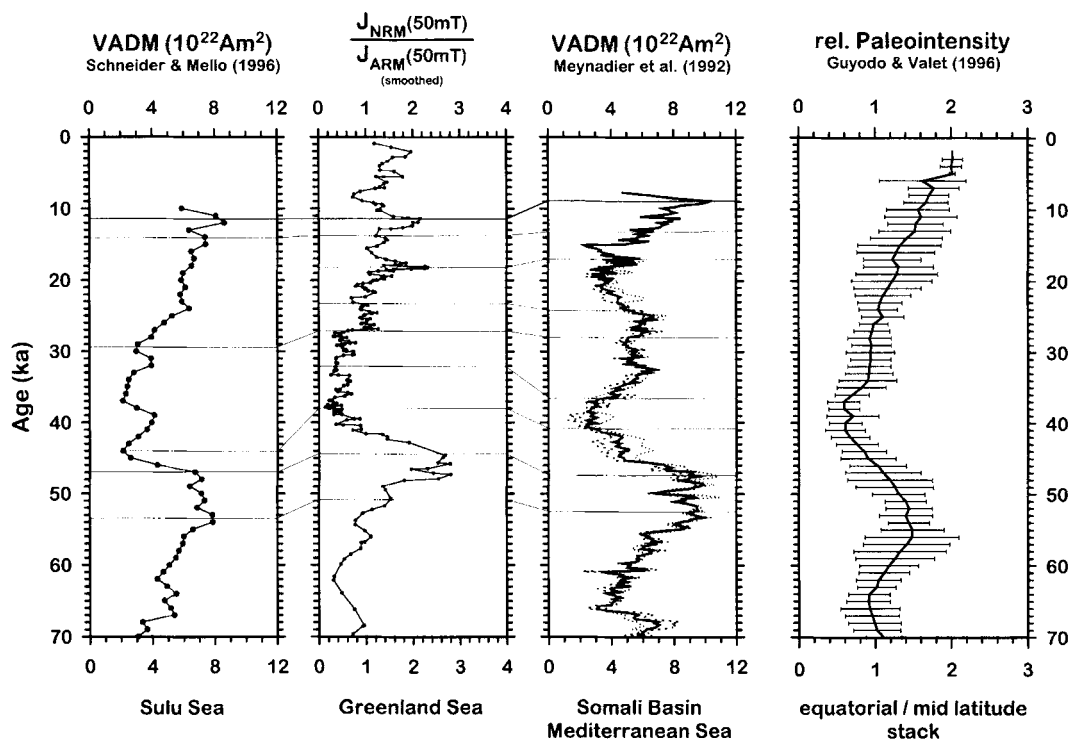


Figure 11. Compilation of different relative palaeointensity records of Schneider & Mello (1996) from the Sulu Sea, the Greenland Sea (this study, smoothing as in Fig. 10), data of Meynadier *et al.* (1992) with a palaeointensity stack (solid line) based on data from the Mediterranean Sea by Tric *et al.* (1992, dashed line) and the Somali Basin (dotted line), together with the stack including standard deviation of Guyodo & Valet (1996) based on 18 different records, mainly from equatorial to mid-latitudes. Data from Schneider & Mello (1996) and Meynadier *et al.* (1992) are included in this stack. VADM—virtual axial dipole moment.

CONCLUSIONS

Rock magnetic investigations on sediments recovered from the Greenland Sea revealed that fine-grained (titano) magnetite is the dominant remanence carrier with not more than *c.* 10 per cent high-coercivity magnetic minerals. Grain-size- and mineralogy-related rock magnetic parameters do not vary significantly across intervals of recorded geomagnetic events. The directional patterns associated with these events therefore represent true geomagnetic field variations. In order to find a good approximation of the relative palaeointensity variations, NRM intensities, after treatment with 50 mT AF peak amplitude, were normalized with the ARM intensity at the same AF level. The results are in good agreement with normalization by the low-field magnetic susceptibility, κ_{LF} , as well as by the SIRM intensities. The recorded geomagnetic events, the Mono Lake excursion (28–27 ka), the Laschamp event (37–33 ka) and the Biwa I/Jamaica event (189–179 ka), are linked to significant minima in the palaeointensity records during the polarity transitions and a slight to moderate increase in intensity during the longer events. In general, the relative palaeointensity record derived from Greenland Sea sediments is in agreement with records obtained from other regions, for example the stack of Guyodo & Valet (1996). This suggests that at least the long-period variations obtained should be due to variations in the dipole moment and that determination of relative palaeointensities can provide a global high-resolution reference database for the correlation of sediment cores.

ACKNOWLEDGMENTS

U. Bleil (University of Bremen, Germany), J. Thiede, and H.-J. Wallrabe-Adams (GEOMAR Kiel, Germany) encouraged this multidisciplinary work. I would also like to thank J.-P. Valet, Y. Guyodo and D. A. Schneider for providing their palaeointensity data and E. Schnepf and T. W. Frederichs for a constructive discussion of the manuscript. The crews of R/V Polarstern are acknowledged for their technical support during cruises ARK V/3a and ARK VII/1. I thank L. Brück for assistance during sampling aboard R/V Polarstern and S. Junek for helping during laboratory work in Potsdam. Tommy McCann kindly corrected the manuscript. The Alfred-Wegener-Institut für Polar- und Meeresforschung provided ship time. This study was partly financed by the Bundesministerium für Forschung und Technologie and by the Deutsche Forschungsgemeinschaft through the SFB 313.

REFERENCES

- Bleil, U. & Gard, G., 1989. Chronology and correlation of Quaternary magnetostatigraphy and nannofossil biostratigraphy in Norwegian-Greenland Sea sediments, *Geol. Rundsch.*, **78**, 1173–1187.
- Bloemendahl, J., King, J.W., Hall, F.R. & Doh, S.-J., 1992. Rock magnetism of late Neogene and Pleistocene deep-sea sediments: relationship to sediment source, diagenetic processes, and sediment lithology, *J. geophys. Res.*, **97**, 4361–4375.
- Bonhommet, N. & Babkine, J., 1967. Sur la présence d'aimantations inversées dans la Chaîne des Puys, *C.R. Acad. Sci. Paris*, **264**, 92–94.

- Cande, S.C. & Kent, D.V., 1995. Revised calibration of the geomagnetic polarity timescale for the Late Cretaceous and Cenozoic, *J. geophys. Res.*, **100**, 6093–6095.
- Chauvin, A., Duncan, R.A., Bonhommet, N. & Levi, S., 1989. Palaeointensity of the earth's magnetic field and K–Ar Dating of the Louchadière volcanic flow (Central France). New evidence for the Laschamp excursion, *Geophys. Res. Lett.*, **16**, 1189–1192.
- Denham, C.R. & Cox, A., 1971. Evidence that the Laschamp polarity event did not occur 13 300–30 400 years ago, *Earth planet. Sci. Lett.*, **13**, 181–190.
- Garnier, F., Herrero-Bevera, E., Laj, C., Guillou, H., Kissel, C. & Thomas, D.M., 1996. Geomagnetic field intensity over the last 42 000 years from core SOH-4, Big Island, Hawaii, *J. geophys. Res.*, **101**, 585–600.
- Guyodo, Y. & Valet, J.-P., 1996. Relative variations in geomagnetic intensity from sedimentary records: the past 200 000 years, *Earth planet. Sci. Lett.*, **143**, 23–36.
- Kawai, N., Yaskawa, K., Nakajima, T., Torii, M. & Horie, S., 1972. Oscillating geomagnetic field with a recurring reversal discovered from Lake Biwa, *Proc. Japan Acad.*, **48**, 186–190.
- King, J.W., Banerjee, S.K., Marvin, J. & Özdemir, Ö., 1982. A comparison of different magnetic methods for determining the relative grain size of magnetite in natural materials: some results from lake sediments, *Earth planet. Sci. Lett.*, **59**, 404–419.
- Levi, S., Audunsson, H., Duncan, R.A., Kristjansson, L., Gillot, P.-Y. & Jakobsson, S.P., 1990. Late Pleistocene geomagnetic excursion in Icelandic lavas: confirmation of the Laschamp geomagnetic excursion, *Earth planet. Sci. Lett.*, **96**, 443–457.
- Løvlie, R., Markussen, B., Sejrup, H.P. & Thiede, J., 1986. Magnetostratigraphy in three Arctic Ocean sediment cores; arguments for geomagnetic excursions within oxygen-isotope stage 2–3, *Phys. Earth planet. Inter.*, **43**, 173–184.
- Meynadier, L., Valet, J.-P., Weeks, R., Shackleton, N.J. & Hagee, V.L., 1992. Relative geomagnetic intensity of the field during the last 140 ka, *Earth planet. Sci. Lett.*, **114**, 39–57.
- Nowaczyk, N.R., 1991. Hochoauflösende Magnetostratigraphie spätquartärer Sedimente arktischer Meeresgebiete (High-resolution magnetostratigraphy of late-Quaternary Arctic marine sediments, engl. abstr.), *Dissertation*, University of Bremen, *Rep. Polar Res.*, **78**.
- Nowaczyk, N.R. & Antonow, M., 1997. High-resolution magnetostratigraphy of four sediment cores from the Greenland Sea—I. Identification of the Mono Lake excursion, Laschamp and Biwa I/Jamaica geomagnetic polarity events, *Geophys. J. Int.*, **131**, 310–324 (this issue).
- Nowaczyk, N.R. & Baumann, M., 1992. Combined high-resolution magnetostratigraphy and nannofossil biostratigraphy for late Quaternary Arctic Ocean sediments, *Deep Sea Res.*, **39**, 567–601.
- Nowaczyk, N.R., Frederichs, T.W., Eisenhauer, A. & Gard, G., 1994. Magnetostratigraphic data from late Quaternary sediments from the Yermak Plateau, Arctic Ocean: evidence for four geomagnetic polarity events within the last 170 Ka of the Brunhes Chron, *Geophys. J. Int.*, **117**, 453–471.
- Roberts, A.P., Verosub, K.L. & Negrini, R.M., 1994. Middle/late Pleistocene relative palaeointensity of the geomagnetic field from lacustrine sediments, Lake Chewaucan, western United States, *Geophys. J. Int.*, **118**, 101–110.
- Roperch, P., Bonhommet, N. & Levi, S., 1988. Paleointensity of the earth's magnetic field during the Laschamp excursion and its geomagnetic implications, *Earth planet. Sci. Lett.*, **88**, 209–219.
- Schneider, D.A., 1993. An estimate of late Pleistocene geomagnetic intensity variation from Sulu Sea sediments, *Earth planet. Sci. Lett.*, **120**, 301–310.
- Schneider, D.A. & Mello, G.A., 1996. A high-resolution marine sedimentary record of geomagnetic intensity during the Brunhes Chron, *Earth planet. Sci. Lett.*, **144**, 297–314.
- Schnepp, E. & Hradetzky, H., 1994. Combined paleointensity and $^{40}\text{Ar}/^{39}\text{Ar}$ age spectrum data from volcanic rocks of the West Eifel field (Germany): Evidence for an early Brunhes geomagnetic excursion, *J. geophys. Res.*, **99**, 9061–9076.
- Smith, J.D. & Foster, J.H., 1969. Geomagnetic reversal in Brunhes normal polarity Epoch, *Science*, **163**, 565–567.
- Stoner, J.S., Channell, J.E.T., Hillaire-Marcel, C., 1995. Late Pleistocene relative geomagnetic paleointensity from the deep Labrador Sea: regional and global correlations, *Earth planet. Sci. Lett.*, **134**, 237–252.
- Tauxe, L., 1993. Sedimentary records of relative paleointensity of the geomagnetic field: Theory and practice, *Rev. Geophys.*, **31** (3), 319–354.
- Tauxe, L. & Shackleton, N.J., 1994. Relative palaeointensity records from the Ontong-Java Plateau, *Geophys. J. Int.*, **117**, 769–782.
- Tauxe, L. & Valet, J.-P., 1989. Relative paleointensity of the earth's magnetic field from marine sedimentary records: a global perspective, *Phys. Earth planet. Inter.*, **56**, 59–68.
- Thouveny, N., 1988. High-resolution palaeomagnetic study of Late Pleistocene sediments from Baffin Bay: first results, *Can. J. Earth Sci.*, **25**, 833–843.
- Tric, E., Valet, J.-P., Tucholka, P., Paterne, M., Labeyrie, L., Guichard, F., Tauxe, L. & Fontugne, M., 1992. Paleointensity of the geomagnetic field during the last 80 000 years, *J. geophys. Res.*, **97**, 9337–9351.
- Valet, J.-P. & Meynadier, L., 1993. Geomagnetic field intensity and reversals during the past four million years, *Nature*, **366**, 234–238.
- Weeks, R.J., Laj, C., Endignoux, L., Mazaud, A., Labeyrie, L., Roberts, A.P., Kissel, C. & Blanchard, E., 1995. Normalised natural remanent magnetisation intensity during the last 240 000 years in piston cores from the central North Atlantic Ocean: geomagnetic field intensity or environmental signal?, *Phys. Earth planet. Inter.*, **87**, 213–229.
- Wollin, G., Ericson, D.B., Ryan, W.B.F. & Foster, J.H., 1971. Magnetism of the earth and climatic changes, *Earth planet. Sci. Lett.*, **12**, 175–183.